Oxygen Storage at the Metal/Oxide Interface of Catalyst Nanoparticles**

Tobias Schalow, Mathias Laurin, Björn Brandt, Swetlana Schauermann, Sebastien Guimond, Helmut Kuhlenbeck, David E. Starr, Shamil K. Shaikhutdinov, Jörg Libuda, and Hans-Joachim Freund*

Numerous processes in chemical industry, in emission control, and in energy technology involve the application of heterogeneous catalysts consisting of nanometer-sized metal particles on high-surface-area oxides.[1,2] Often, it is found that the activity of these so-called supported catalysts critically depends not only on the size and morphology of the metal particles, but also on the support itself. At the microscopic level, the origins of such effects are poorly understood in most cases. The situation turns out to be particularly intricate for the case of oxidation reactions on supported transition-metal particles. Here, many different oxygen species may be present under reaction conditions, for example, different types of chemisorbed oxygen, subsurface oxygen, surface oxides, and bulk oxides (see e.g. Refs. [3–16] and references therein). On some transition metals such as Ru, it has indeed been shown that not the metal surface itself but surface oxides formed under reaction conditions may represent the active phase of the catalyst.[17] Also for Pd surfaces strong changes in activity have recently been observed at higher partial pressures and have been related to surface oxidation processes (Ref. [18], see also Refs. [19,20]). In most cases, however, it is unclear what the role of the different oxygen species may be during oxidation reactions.

In this contribution, we suggest a new mechanism for oxygen storage and oxidation on oxide-supported metal catalysts: For a Pd/Fe_3O_4 model catalyst it is shown that large amounts of oxygen can be reversibly accumulated in form of a thin Pd oxide layer at the metal/oxide interface. From this interface oxide layer, which is stabilized by the support, oxygen is released and migrates back onto the metallic Pd surface, where it then is available for oxidation reactions. This storage mechanism may play an important role for the kinetics of oxidation reactions, in particular under non-steady-state conditions.

The experimental approach leading to these insights is summarized in Figure 1: Briefly, we employ well-defined supported model catalysts, which are characterized in detail by surface-science methods. These systems are then probed with respect to their reactivity using molecular beam techniques. The use of model systems is motivated by the high degree of complexity of real catalysts and by experimental restrictions concerning the application of surface-science methods to these systems. Both points often preclude detailed insights into the surface chemistry and structure of real catalysts. Supported model catalysts, on the other hand, provide clean and well-defined surfaces with strongly reduced complexity and are easily accessible for most experimental techniques available in surface science.[21–23]

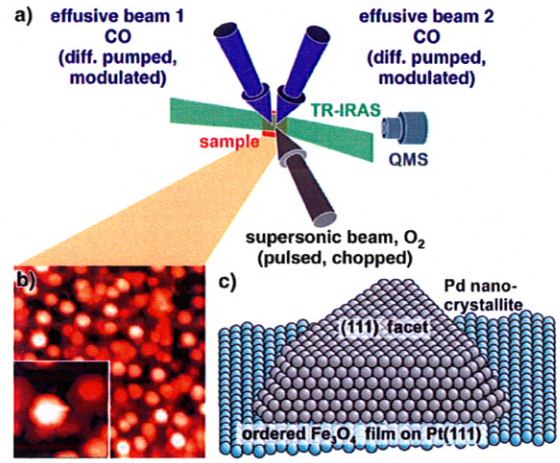

Figure 1. a) Representation of the molecular beam setup; b) STM image (100 nm × 100 nm, inset: 20 nm × 20 nm) of the Pd nanoparticles on Fe_3O_4/Pt(111) (after annealing at 600 K and oxidation and reduction at 500 K); c) model of the Pd nanoparticles.

In this study, we used Pd nanoparticles grown by metal-vapor deposition on a thin, well-ordered Fe_3O_4 film on Pt(111). The model catalyst was prepared in situ under ultrahigh-vacuum (UHV) conditions. Structure, morphology, and adsorption properties of both the Fe_3O_4 support[24,25] and the Pd particles were previously investigated in detail.[26] In Figure 1b a scanning tunnelling microscopy (STM) image of the Pd particles is shown as well as a model schematically illustrating their morphology. The three-dimensional particles have an average diameter of approximately 7 nm and contain around 3000 Pd atoms per particle. They are characterized by a well-defined crystalline shape, grow in (111) orientation with respect to the substrate, and expose a majority of (111) as well as a smaller fraction of (100) sites.

In order to study the interaction of the supported model catalyst with oxygen, we employed molecular beam (MB) methods. Molecular beams are well-established among the major experimental tools to study surface kinetics and dynamics[27–29] (for some recent examples in model catalysis see Refs. [30–32]). In this work, the technique is utilized to

[*] Dipl.-Ing. T. Schalow, Dipl.-Chem. M. Laurin, Dipl.-Chem. B. Brandt, Dipl.-Chem. S. Schauermann, Dipl.-Chem. S. Guimond, Dr. H. Kuhlenbeck, Dr. D. E. Starr, Dr. S. K. Shaikhutdinov, Priv.-Doz. Dr. J. Libuda, Prof. Dr. H.-J. Freund
Fritz-Haber-Institut der Max-Planck-Gesellschaft
Faradayweg 4–6, 14195 Berlin (Germany)
Fax: (+49) 30-8413-4309
E-mail: libuda@fhi-berlin.mpg.de

[**] This work has been funded by the Deutsche Forschungsgemeinschaft (SPP 1091) and the Fonds der Chemischen Industrie. The authors are particularly grateful to the BESSY staff for technical support.

quantitatively determine the oxygen uptake and release under exactly controlled and isothermal conditions. The MB apparatus used allows us to superimpose up to three independent reactant beams on the sample surface and facilitates simultaneous gas-phase detection (quadrupole mass spectrometry, QMS) and surface spectroscopy (time-resolved IR reflection absorption spectroscopy, TR-IRAS, see Figure 1 a).[33]

To quantitatively probe the oxygen uptake and release we performed pulsed CO titration experiments as shown in Figure 2: First, the model surface was exposed to a pulse of oxygen. After a defined delay time, short pulses of CO were applied in order to probe oxygen release by means of oxidation of CO to CO_2. The latter desorbs immediately and can be detected in the gas phase. In all experiments a supersonic beam of $^{18}O_2$ was employed in order to minimize the background signal. Experimentally, this type of pulsed titration technique allows an exact quantification of the CO_2 yield, even at very low reaction rates.

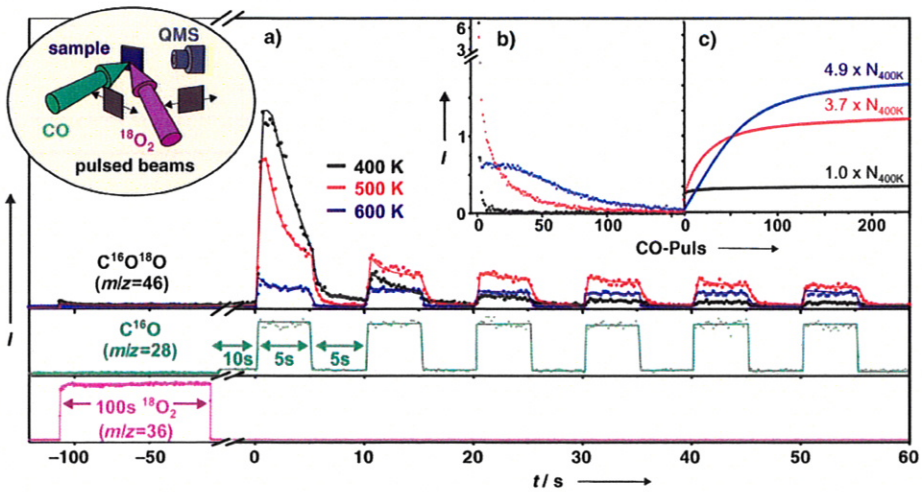

Figure 2. Pulsed CO titration experiment on the Pd/Fe_3O_4 model catalyst after oxygen exposure at different sample temperatures. Initially the model surface is exposed to a pulse of $^{18}O_2$ (100 s). After a delay time (10 s), pulses of CO (on-time 5 s, off-time 5 s) are applied to remove oxygen stored on the catalyst surface in form of CO_2: a) CO_2 formation rate; b) CO_2 yield per CO pulse; c) total CO_2 yield.

Pulsed titration experiments were performed as a function of surface temperature. At 400 K we find very high initial reaction rates, which drop to the background level within few CO pulses. The observations indicate high initial reaction probabilities and low oxygen uptake. This type of behavior is consistent with the presence of solely chemisorbed oxygen on the Pd particles and agrees well with what is expected on the basis of previous studies.[34–36] (The expected coverages of atomic oxygen would be around 0.25 monolayers (ML) on Pd(111) and around 0.5 ML on Pd(100), see Refs. [9,12] and references therein).

With increasing oxidation temperature (500–600 K) a surprising behavior is observed: The CO_2 formation rate in the first CO pulse decreases, but subsequently the rate remains finite for a long time, that is, up to 50 to 100 CO pulses. Simultaneously, the total CO_2 yield, obtained by integrating over all pulses (see Figure 2 b,c), increases drastically, indicating a nearly fivefold increase in the total oxygen release between 400 K and 600 K. Two conclusions can be drawn from these observations:

a) Partial surface oxidation of metal particles: The large oxygen release cannot be explained by surface chemisorption only. Alternatively, oxygen uptake and release by means of oxidation and reduction of the Fe_3O_4 support could be invoked. However, titration experiments on isotopically labeled supports show that oxygen exchange with the support is very slow under the experimental conditions applied in this work.[37] Therefore, we attribute the storage effect to the formation of a thin oxide layer on the Pd particles. It is well established that on Pd single crystals surface oxides can be formed under similar conditions.[10–16] Recently detailed structure models for surface oxides on both Pd(111)[13] and Pd(100)[14] were suggested on the basis of combined theoretical and experimental work. The oxygen densities in surface oxides drastically exceeds those in chemisorbed layers, allowing oxygen storage and subsequent release.[38] It is expected, however, that the oxidation behavior of small supported particles may differ from the behavior observed on single-crystal surfaces. Differences may arise, for example, from the simultaneous presence of different types of facets and low coordinated sites, from lattice distortions, and from the particle support interface. As will be discussed in a forthcoming publication,[37] the process of surface oxidation can be monitored and analyzed in detail by means of IRAS using CO as a probe molecule. For the work discussed here, the most important point to note is that metallic and oxidized surface areas coexist on the Pd particles over a large temperature region, ranging from approximately 450 K to 600 K. Within this temperature region the fraction of the metallic part decreases with increasing oxidation temperature.

b) Reactivity of partially oxidized metal particles: The low initial reaction rate after oxidation at 600 K shows that the CO reaction probability on the surface oxide is drastically lower than on the metallic surface. Consequently, for a partially oxidized surface the CO_2 yield of the first CO pulse can be interpreted as the amount of chemisorbed oxygen adsorbed on the metallic part of the Pd particles. With increasing oxidation temperatures, the amount of chemisorbed oxygen decreases as a result of the increasing fraction of the surface covered by the oxide. This result fits well with IRAS work mentioned above, showing that after oxidation at 600 K a major fraction of the particle surface is covered by surface oxides, whereas after oxidation at

500 K only a minor part is oxidized. Accordingly, the CO_2 yield of the following CO pulses can be assigned to CO oxidation involving oxygen originating from the oxide layer. Two points are noteworthy here: Firstly, the amount of oxygen stored at 500 K is large in spite of the small degree of surface oxidation (see Figure 2c)). As shown below, this effect can be attributed to a preferential oxidation of the particle/support interface. Secondly, the CO_2 yield per pulse is initially higher at lower surface oxide coverage (500 K oxidation) than at higher coverage (600 K oxidation). This finding indicates that CO does not react directly with surface oxide. Instead, we suggest that the reduction mechanism proceeds predominantly by slow decomposition of the oxide, releasing oxygen onto the metallic Pd parts, where it readily reacts with coadsorbed CO. This model is in agreement with a detailed analysis of the transient behavior of pulsed CO titration experiments.[37] We conclude that the surface oxide layer, covering part of the particle surface, acts as an oxygen reservoir allowing storage and release of oxygen in a reversible fashion.

In view of the above results showing partial oxidation of the Pd surface, the question arises which parts of the nanoparticle are initially oxidized and, therefore, are primarily responsible for the oxygen-storage mechanism. To address these questions we have performed high-resolution photoelectron spectroscopy (PES) using synchrotron radiation (see Figure 3). For the clean Pd particles before exposure to oxygen, the Pd $3d_{5/2}$ region contains two features: a Pd bulk signal (binding energy, BE = 335.0–335.1 eV) and a surface- and interface-derived component (BE = 335.3–335.6 eV) (compare e.g. Refs. [13, 14]). The surface sensitivity of the experiment can be varied by changing the photon energy. With increasing photon energy ($h\nu$) the kinetic energy of the photoelectrons increases and so does the electron escape length λ ($h\nu = 465$ eV, $\lambda \approx 4$ Å; $h\nu = 840$ eV, $\lambda \approx 9$ Å[39]). As a result, the bulk feature becomes more prominent at higher photon energy, that is, at a lower degree of surface sensitivity.

After oxidation at 600 K (at similar oxygen doses as those in MB experiments), components at higher BE are observed, which are characteristic for oxygen chemisorption and surface oxidation. Based on high-resolution PES work on single-crystal surfaces,[13,14] the Pd $3d_{5/2}$ region can be qualitatively decomposed into three regions: 1) a low BE component (335.0–335.1 eV) related to bulk Pd metal, 2) an intermediate BE region (around 335.7 eV) containing contributions from metallic Pd coordinated to chemisorbed oxygen and from specific Pd atoms in thin oxide layers, and 3) a high BE region (around 336.6–336.7 eV) due to Pd atoms in thin oxide layers only. A more detailed assignment is precluded by the large number of nonequivalent Pd atoms, exposed by the supported particle system.

Two main conclusions can be drawn from the spectra. First, the constant BE of the Pd bulk feature upon oxidation indicates that the metallic nature of the particle core is preserved and rules out significant dissolution of oxygen in the Pd lattice, the latter result being in agreement with recent theoretical studies.[16] The most surprising observation, however, is the decreasing intensity of the metallic bulk signal with increasing photon energy (similar effects also observed at other photon energies and oxidation temperatures). This finding indicates that the Pd oxide layer is not preferentially formed on the outer particle surface, that is, at the Pd/vacuum interface, but rather below the particles, that is, at the metal/support interface. As a driving force for preferential formation of a Pd interface oxide we suggest that the oxide film is stabilized by interaction with the iron oxide support. Further evidence for this hypothesis is derived from transient MB experiments showing that there is a dynamic equilibrium between chemisorbed oxygen on the metallic Pd and the interface oxide, strongly favoring formation of the latter.[37] This observation is in contrast to the oxidation behavior of Pd single crystals, on which surface-oxide formation occurs at high oxygen coverage only.[16] Finally, it should be noted that the formation of a Pd interface oxide is in agreement with the MB and IRAS experiments discussed above, showing that at 500 K substantial oxygen storage occurs without a pronounced loss of the metallic Pd surface.

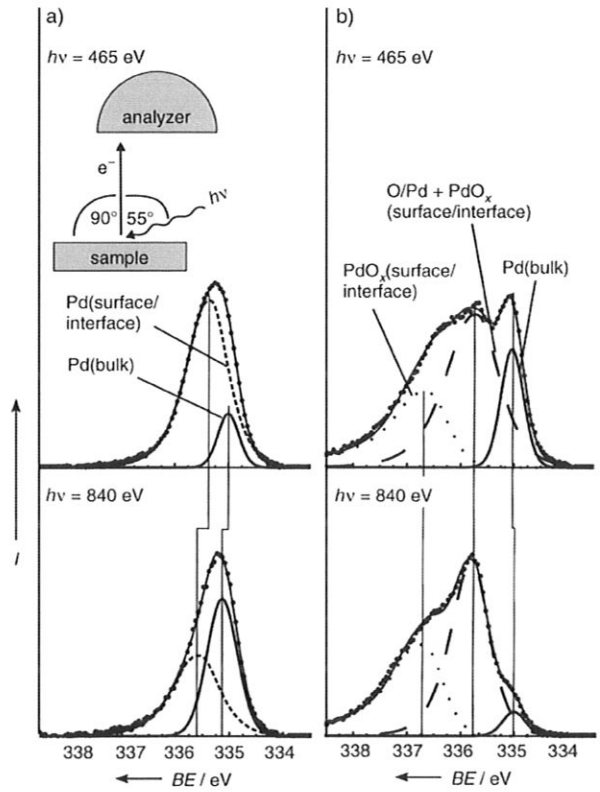

Figure 3. High-resolution core-level spectra of Pd $3d_{5/2}$ region after preparation of the model catalyst at different photon energies: a) immediately after Pd deposition and annealing in UHV to 600 K; b) after oxygen exposure at 600 K (oxygen dose: 3×10^{17} molecules cm^{-2}).

A schematic summary of our proposed oxygen-storage and CO-oxidation mechanism is depicted in Figure 4: We have shown that for a Pd/Fe_3O_4 model catalyst reversible oxygen storage and release occurs at 500 K and above through formation of thin Pd oxide layers. Preferentially the

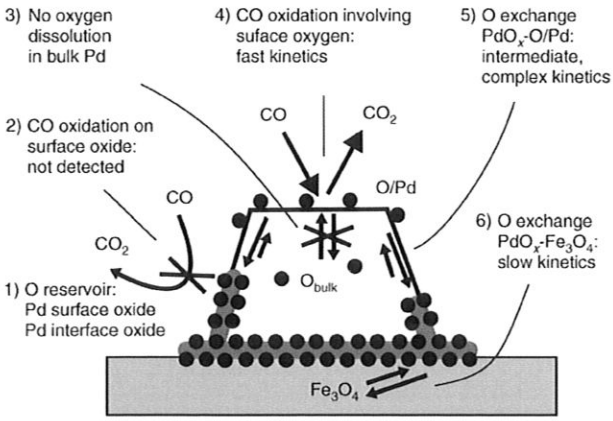

Figure 4. Illustration of the oxygen storage and CO oxidation mechanism on the Pd/Fe_3O_4-supported model catalyst.

oxide layer forms at the particle/support interface due to stabilization by the Fe_3O_4 support, before—under more drastic conditions—oxidation of the complete particle surface occurs. A dynamic equilibrium is established between oxygen chemisorbed on the metal and oxygen incorporated into the interface or surface oxides. As a result, the oxide layers can act as an oxygen reservoir for oxidation reactions. For the specific case of CO oxidation, the reaction with chemisorbed oxygen on metallic Pd is fast, whereas the reaction probability on the surface oxide is low. Thus CO oxidation occurs by release of oxygen from the interface oxide onto the metal surface, where it subsequently reacts with coadsorbed CO. Large amounts of oxygen can be stored and released by this mechanism, without substantial changes of the metal surface available. It may be anticipated that similar storage mechanisms might be active for other dispersed metal catalysts on reducible or irreducible oxide supports as well.

Experimental Section

MB and IRAS experiments were performed in a UHV apparatus at the Fritz-Haber-Institut (Berlin) which allows up to three beams to be crossed on the sample surface.[33] The CO beam (Linde, 99.997%, further purified by a gas filter (Mykrolis)) was generated by a doubly differentially pumped effusive multichannel array source and modulated by a motorized shutter. The $^{18}O_2$ beam (Campro Scientific, 95% ^{18}O, 99.7% purity) was generated from a triply differentially pumped supersonic expansion and modulated using a solenoid valve. Typical intensities of the beams were 2.1×10^{14} molecules $cm^{-2}s^{-1}$ for CO and 4.6×10^{14} molecules $cm^{-2}s^{-1}$ for O_2. For measuring the reaction rate, an automated QMS system (ABB Extrel) was employed. PES was performed at BESSY II, Beamline UE52-PGM1 with a 200-mm hemispherical energy analyzer (Scienta SES200). The energy resolution was approximately 100 meV at $h\nu = 465$ eV and 160 meV at $h\nu = 840$ eV.

The thin (≈ 100 Å) Fe_3O_4 film was grown on Pt(111) by repeated cycles of Fe (>99.99%, Goodfellow) deposition and subsequent oxidation (see Refs. [24–26] for details). Cleanliness and quality of the oxide film was checked by IRAS of adsorbed CO (for MB experiments) and low-energy electron diffraction. Pd particles (>99.9%, Goodfellow) were grown by physical vapor deposition (Pd coverage: 2.7×10^{15} atoms cm^{-2}, sample temperature: 100 K) using a commercial evaporator (Focus, EFM 3, flux calibrated by a quartz microbalance). The particles were stabilized by annealing to 600 K in UHV and subsequent oxidation/reduction cycles at 500 K.

[1] G. Ertl, H. Knoezinger, J. Weitkamp in *Handbook of Heterogeneous Catalysis* (Eds.: G. Ertl, H. Knoezinger, J. Weitkamp), VCH, Weinheim, **1997**.
[2] J. M. Thomas, W. J. Thomas, *Principle and Practice of Heterogeneous Catalysis*, VCH, Weinheim, **1997**.
[3] H. Conrad, G. Ertl, J. Küppers, E. E. Latta, *Surf. Sci.* **1977**, *65*, 235.
[4] R. Imbihl, J. E. Demuth, *Surf. Sci.* **1986**, *173*, 395.
[5] S.-L. Chang, P. A. Thiel, *J. Chem. Phys.* **1988**, *88*, 2071.
[6] X. Guo, A. Hoffman, J. T. Yates, Jr., *J. Chem. Phys.* **1989**, *90*, 5787.
[7] V. A. Bondzie, P. Kleban, D. J. Dwyer, *Surf. Sci.* **1996**, *347*, 319.
[8] E. H. Voogt, A. J. M. Mens, J. W. G. O. L. J. Gijzeman, *Surf. Sci.* **1997**, *373*, 210.
[9] F. P. Leisenberger, G. Koller, M. Sock, S. Surnev, M. G. Ramsey, F. P. Netzer, B. Klötzer, K. Hayek, *Surf. Sci.* **2000**, *445*, 380.
[10] V. A. Bondzie, P. H. Kleban, D. J. Dwyer, *Surf. Sci.* **2000**, *465*, 266.
[11] G. Zheng, E. I. Altman, *Surf. Sci.* **2000**, *462*, 151.
[12] G. Zheng, E. I. Altman, *Surf. Sci.* **2002**, *504*, 253.
[13] E. Lundgren, G. Kresse, C. Klein, M. Borg, J. N. Andersen, M. De Santis, Y. Gauthier, C. Konvicka, M. Schmid, P. Varga, *Phys. Rev. Lett.* **2002**, *88*, 246103.
[14] M. Todorova, E. Lundgren, V. Blum, A. Mikkelsen, S. Gray, J. Gustafson, M. Borg, J. Rogal, K. Reuter, J. N. Andersen, M. Scheffler, *Surf. Sci.* **2003**, *541*, 101.
[15] E. Lundgren, J. Gustafson, A. Mikkelsen, J. N. Andersen, A. Stierle, H. Dosch, M. Todorova, J. Rogal, K. Reuter, M. Scheffler, *Phys. Rev. Lett.* **2004**, *92*, 046101.
[16] M. Todorova, K. Reuter, M. Scheffler, *Phys. Rev. B* **2005**, *71*, 195403.
[17] H. Over, Y. D. Kim, A. P. Seitsonen, S. Wendt, E. Lundgren, M. Schmid, P. Varga, A. Morgante, G. Ertl, *Science* **2000**, *287*, 1474.
[18] B. L. M. Hendriksen, S. C. Bobaru, J. W. M. Frenken, *Surf. Sci.* **2004**, *552*, 229.
[19] M. R. Basset, R. Imbihl, *J. Chem. Phys.* **1990**, *93*, 811.
[20] J. Hartmann, R. Imbihl, W. Vogel, *Catal. Lett.* **1994**, *28*, 373.
[21] C. R. Henry, *Surf. Sci. Rep.* **1998**, *31*, 231.
[22] H.-J. Freund, M. Bäumer, J. Libuda, T. Risse, G. Rupprechter, S. Shaikhutdinov, *J. Catal.* **2003**, *216*, 223.
[23] D. W. Goodman, *J. Catal.* **2003**, *216*, 213.
[24] W. Weiss, W. Ranke, *Prog. Surf. Sci.* **2002**, *70*, 1.
[25] C. Lemire, R. Meyer, V. Henrich, S. K. Shaikhutdinov, H.-J. Freund, *Surf. Sci.* **2004**, *572*, 103.
[26] R. Meyer, S. K. Shaikhutdinov, H.-J. Freund, *Z. Phys. Chem.* **2004**, *218*, 2004.
[27] M. P. D'Evelyn, R. J. Madix, *Surf. Sci. Rep.* **1984**, *3*, 413.
[28] C. T. Rettner, D. J. Auerbach, *J. Chem. Phys.* **1996**, *105*, 8842.
[29] A. W. Kleyn, *Chem. Soc. Rev.* **2003**, *32*, 87.
[30] S. Schauermann, J. Hoffmann, V. Johánek, J. Hartmann, J. Libuda, H.-J. Freund, *Angew. Chem.* **2002**, *114*, 2643; *Angew. Chem. Int. Ed.* **2002**, *41*, 2532.
[31] V. Johanek, S. Schauermann, M. Laurin, J. Libuda, H.-J. Freund, *Angew. Chem.* **2003**, *115*, 3143; *Angew. Chem. Int. Ed.* **2003**, *42*, 3035.
[32] J. Libuda, H.-J. Freund, *Surf. Sci. Rep.*, in press.

[33] J. Libuda, I. Meusel, J. Hartmann, H.-J. Freund, *Rev. Sci. Instrum.* **2000**, *71*, 4395.
[34] T. Engel, G. Ertl, *J. Chem. Phys.* **1978**, *69*, 1267.
[35] L. Piccolo, C. Becker, C. R. Henry, *Appl. Surf. Sci.* **2000**, *164*, 156.
[36] J. Libuda, I. Meusel, J. Hoffmann, J. Hartmann, L. Piccolo, C. R. Henry, H.-J. Freund, *J. Chem. Phys.* **2001**, *114*, 4669.
[37] T. Schalow, B. Brandt, M. Laurin, J. Libuda, H.-J. Freund, in preparation.
[38] G. Zheng, E. I. Altmann, *J. Phys. Chem. B* **2002**, *106*, 1048.
[39] S. Tanuma, C. J. Powell, D. R. Penn, *Surf. Interface Anal.* **1991**, *17*, 927.